Ersch. in: Journal of Organometallic Chemistry ; 534 (1997), 1-2. - S. 67-79

http://dx.doi.org/10.1016/S0022-328X(96)06895-7

ansa-Metallocene derivatives XXXVI. [1] Dimethylsilyl-bridged permethyl chromocene carbonyl complexes – syntheses, crystal structures and interconversion reactions [2]

Frank Schaper, Marcus Rentzsch, Marc-Heinrich Prosenc, Ursula Rief, Katrin Schmidt, Hans-Herbert Brintzinger *

Fakultät für Chemie, Universität Konstanz, Postfach 5560, D-78434 Konstanz, Germany

Abstract

The ring-bridged chromocene carbonyl complex $Me_2Si(C_5Me_4)_2Cr(CO)$ **1** is obtained by reaction of $Me_2Si(C_5Me_4)_2Li_2$ with $CrCl_2 \cdot THF$ in the presence of CO. Reaction with CO transforms the monocarbonyl complex **1** to a dicarbonyl complex $Me_2Si(C_5Me_4)(C_5(endo\text{-}3\text{-}H)(2\text{-}CH_2)Me_3)Cr(CO)_2$ **2**; in this reaction, a hydrogen atom is shifted from one of the α-CH_3 groups to the adjacent β-position of a C_5 ring ligand. The rate of this reaction is first order in complex and CO concentration, with an activation enthalpy of $H^{\neq} = 51 \pm 3\,kJ\,mol^{-1}$ and an activation entropy of $S^{\neq} = 136 \pm 10\,J\,mol^{-1}\,K^{-1}$. In toluene solution at 50 °C, complex **2** isomerizes to $Me_2Si(C_5Me_4)(C_5(exo\text{-}3\text{-}H)(2\text{-}CH_2)Me_3)Cr(CO)_2$ **3**, then to $Me_2Si(C_5Me_4)(C_5(exo\text{-}1\text{-}H)(2\text{-}CH_2)Me_3)Cr(CO)_2$ **4** and further to $Me_2Si(C_5Me_4)(C_5(endo\text{-}5\text{-}H)(2\text{-}CH_2)Me_3)Cr(CO)_2$ **5**. The kinetics of these isomerizations, which involve hydrogen migrations and ring rotation reactions, indicate monomolecular reactions. Possible reaction paths and transition states are discussed. The structures of complexes **1–5** were determined by ^1H NMR spectroscopy, those of **1**, **2**, **4** and **5** also by single-crystal X-ray diffraction. Complex **1**: space group $P2_1/n$, $a = 13.257(7)$ Å, $b = 10.186(5)$ Å, $c = 14.739(7)$ Å, $\beta = 90.89(4)°$; $V = 1990.1(7)$ Å^3; $Z = 4$. Complex **2**: space group $Pbca$, $a = 8.699(3)$ Å, $b = 14.713(6)$ Å, $c = 32.801(14)$ Å; $V = 4198(3)$ Å^3; $Z = 8$. Complex **4**: space group $P2_1$, $a = 9.497(2)$ Å, $b = 9.895(3)$ Å, $c = 11.371(2)$ Å, $\beta = 103.919(8)°$; $V = 1037.1(4)$ Å^3; $Z = 2$. Complex **5**: space group $P2_1/c$, $a = 16.555(4)$ Å, $b = 13.036(3)$ Å, $c = 10.044(2)$ Å, $\beta = 107.45(1)°$; $V = 2067.8(8)$ Å^3; $Z = 4$.

Keywords: Carbonyl complexes; Chromium; Dimethylsilyl bridge; Hydrogen transfer; Metallocene; Rearrangement

1. Introduction

The role of Group 4 metallocene complexes in recently developed homogeneous polymerisation catalysts, as well as that of molybdenum nitrosyl and carbonyl complexes in homogeneous metathesis catalysts, has been elucidated in great part by spectroscopic and kinetic studies originating from Taube's research group [2].

Compared to this rich chemistry of their Group 4 and Group 6 metallocene analogues, chromocene derivatives have a rather limited range of reactivities: low-spin complexes of the type $(C_5H_5)_2Cr$–L, if formed at all [3], are thermally much less stable than the analogous species Cp_2M–L with M = Mo, W [4]. Upon oxidation of $(C_5R_5)_2Cr$ (R = H, Me), one obtains axially symmetric chromocenium ions, $(C_5R_5)_2Cr^+X^-$ ($X^- = I^-$, I_3^-) without a Cr–X bond [5–7], instead of the tetracoordinate species $(C_5R_5)_2MXY$ typical for Group 4 and other Group 6 metallocene complexes [8]. Complexes of the type $(C_5H_5)_2CrXY$ with X,Y = halogen or pseudohalogen have been reported to form from $(C_5H_5)_2Cr$ and XY, no structural data are available for these complexes however [9].

In previous studies, we have shown that an interannular ethano bridge provides the carbonyl complex $Me_4C_2(C_5H_4)_2Cr(CO)$ with a thermal stability comparable to that of $(C_5H_5)_2Mo(CO)$ or $(C_5H_5)_2W(CO)$ [10,11]. The increased stability of these ring-bridged

* Corresponding author.

[1] For Part 35 see Ref. [1].

[2] Dedicated to Professor Rudolf Taube on the occasion of his 65th birthday.

complexes has been analyzed in terms of complex deformation and metal–ligand bond enthalpies [12]. The Me_4C_2-bridged chromocene carbonyl resembles $(C_5H_5)_2W(CO)$ also in that it is converted, at elevated CO pressures, to the dicarbonyl complex $Me_4C_2(C_5H_4)_2Cr(CO)_2$ with one η^3- and one η^5-bound C_5 ring [13]. Similar effects result when permethylated C_5 rings make the Cr centre more electron-rich: while the dicarbonyl complex $(C_5H_5)_2Cr(CO)_2$ is stable only under elevated CO pressures [13], its permethyl analogue η^5,η^3-$(C_5Me_5)_2Cr(CO)_2$ can be isolated by sublimation in vacuo [14]. It appeared worthwhile, therefore, to investigate the reactivity of chromocene complexes that are ring-bridged as well as permethylated. Here we report on the synthesis and structures of complexes of the type $Me_2Si(C_5Me_4)_2Cr(CO)_x$, with $x = 1$, 2, and on their interconversion reactions.

2. Results and discussion

2.1. Formation and structure of $Me_2Si(C_5Me_4)_2Cr(CO)$ 1

The dilithium salt $Me_2Si(C_5Me_4)_2Li_2$, prepared with some modifications according to previous reports [15–17], reacts with $CrCl_2 \cdot THF$ in THF solution to give only insoluble, red precipitates, probably polymeric Me_2Si-linked chromocene derivatives. Similar observations were reported for the reaction of $Me_4C_2(C_5H_4Li)_2$ with $CrCl_2 \cdot THF$ [10]. Analogous reactions in the presence of CO, however, give the red-brown complex $Me_2Si(C_5Me_4)_2Cr(CO)$ **1** after crystallization from pentane, in yields of ca. 40%. Analogous reactions of $H_4C_2(C_5Me_4Li)_2$ [17] with $CrCl_2 \cdot x$THF under CO give a green complex $H_4C_2(C_5Me_4)_2Cr(CO)$ with ν(CO) 1883 cm^{-1} (toluene). Similarly, $Me_2Si(C_5Me_4)_2Li_2$ reacts with $CrCl_2 \cdot x$THF in the presence of PMe_3 to give a green product with four ^1H NMR signals in the range δ 0.52 to 2.05, as expected for a C_{2v}-symmetric phosphine complex $Me_2Si(C_5Me_4)_2Cr(PMe_3)$. Neither of these complexes could be completely characterized, however. While this work was in progress, an alternative synthetic access to the *ansa*-chromocene monocarbonyl complex $Me_4C_2(C_5H_4)_2Cr(CO)$, from calcocene as starting material, has been reported [18].

The ^1H NMR spectrum of complex **1** (see Section 4) is in accord with the expected C_{2v}-symmetry. Its ν(CO) frequency of 1876 cm^{-1} (toluene) is intermediate between those of chromocene carbonyl complexes with C_2H_4-bridged [10] and permethylated C_5 rings [13] (Table 1). In its EI mass spectrum, the parent peak M^+ at m/e 378 is rather weak; loss of CO gives rise to the base peak $[M - CO]^+$.

Complex **1** crystallizes from pentane solution in the form of deep-blue cubes, suitable for an X-ray diffraction study (see Section 4). The molecular structure (Fig. 1) is close to C_{2v}-symmetry; the Cr–C–O bond angle is 178.5° and the Cr–CO bond deviates only by 0.7° from the Cr–Si axis. Cr–C_5 distances are between 215 and 222 pm, the Cr–C(*ipso*) distance being smaller by ca. 6–7 pm than the Cr–C(β) distance (Table 2).

Table 1
Wavenumbers of the CO stretching vibration $\tilde{\nu}$(CO) (cm^{-1})

$(C_5Me_5)_2Cr(CO)$ [a,b]	1857
$Me_2Si(C_5Me_4)_2Cr(CO)$ **1** [a]	1876
$Me_4C_2(C_5H_4)_2Cr(CO)$ [a,c]	1905
$(\eta^5$-$C_5Me_5)(\eta^3$-$C_5Me_4)Cr(CO)_2$ [a,b]	1903, 1840
$Me_2Si(C_5Me_4)(C_5$(*endo*-3-H)(2-CH_2)$Me_3)Cr(CO)_2$ **2** [a]	1924, 1858
$Me_2Si(C_5Me_4)(C_5$(*exo*-1-H)(2-CH_2)$Me_3)Cr(CO)_2$ **4** [a]	1910, 1845
$Me_2Si(C_5Me_4)(C_5$(*endo*-5-H)(2-CH_2)$Me_3)Cr(CO)_2$ **5** [a]	1926, 1861
$Me_4C_2(\eta^5$-$C_5H_4)(\eta^3$-$C_5H_4)Cr(CO)_2$ [a,b]	1939, 1875
$(\eta^5$-$C_5H_4)(\eta^3$-$C_5H_7)Cr(CO)_2$ [d]	1916, 1835

[a] In toluene.
[b] Ref. [13]; [c] Ref. [10]; [d] Ref. [19].

Remarkable is a deviation of the Si–C(*ipso*) bonds by 27–28° from the mean plane of the adjacent C_5 ring (Table 3). While out-of-plane deformations at the *ipso*-C atoms will necessarily be found in Me_2Si-bridged metallocenes, this deformation is much larger here than the 9–15° observed e.g. for Me_2Si-bridged zirconocenes [20]. The Si centre with a C(*ipso*)–Si–C(*ipso*) angle of 91.7° also deviates substantially from tetrahedral geometry. Apparently, the relatively small Cr atom does not fit adequately into the intrinsically rather open Me_2Si-bridged ligand framework.

2.2. Formation and structure of $Me_2Si(C_5Me_4)(C_5HMe_3CH_2)Cr(CO)_2$ 2

In addition to complex **1**, reactions of $Me_2Si(C_5Me_4)_2Li_2$ with $CrCl_2 \cdot THF$ under CO also

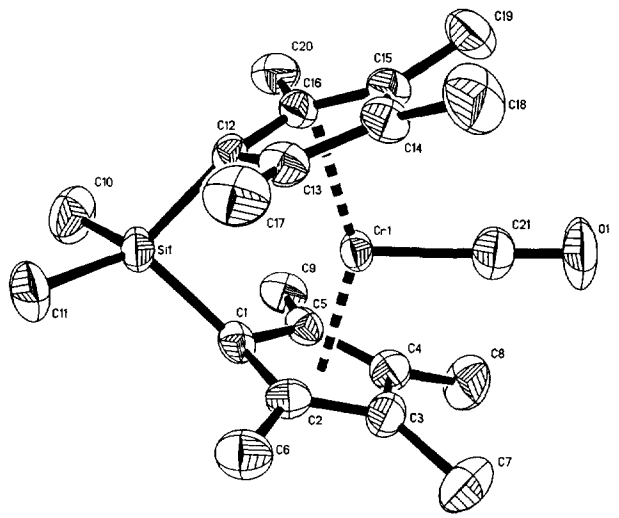

Fig. 1. Crystal structure of the monocarbonyl complex **1**. Thermal ellipsoids are drawn at the 50% probability level. Hydrogen atoms are omitted for clarity.

Table 2
Selected bond lengths (pm)

	1	2	4	5
Cr–C1	214.5(5)	219.8(6)	218.5(2)	218.6(2)
Cr–C2	217.6(5)	215.3(8)	219.4(2)	214,8(2)
Cr–C3	220.9(5)	218.6(9)	223.8(2)	218.8(3)
Cr–C4	222.0(5)	223.7(9)	223.8(2)	222.0(2)
Cr–C5	215.6(5)	225.0(9)	220.3(2)	224.3(3)
Cr–X1	180.8 [a]	184.4 [a]	185.2 [a]	183.4 [a]
Cr–C12	215.9(4)	240.9(8)	189.9(2)	235.7(2)
Cr–C13	217.1(5)	—	—	—
Cr–C14	220.1(5)	—	—	—
Cr–C15	221.1(5)	—	241.6(2)	—
Cr–C16	217.1(5)	222.3(7)	218.2(2)	221.7(2)
Cr–C20	—	219.2(7)	220.8(2)	219.9(2)
Cr–X2	180.9 [b]	201.1 [c]	201.1 [d]	199.5 [c]
Cr–C21	184.4(6)	181.3(8)	182.6(2)	182.3(3)
C21–O1	116.3(8)	116.1(10)	115.3(3)	114.9(3)
Cr–C22	—	180.1(9)	180.4(2)	183.3(3)
C22–O2	—	118.5(11)	115.9(3)	115.0(3)
O1–C2	144.8(6)	146.0(11)	143.2(3)	144.5(4)
C2–C3	142.1(7)	140.4(12)	142.6(3)	142.0(4)
C3–C4	143.3(7)	142.6(11)	140.5(3)	141.6(4)
C3–C7	150.9(8)	150.3(12)	149.5(3)	149.5(4)
C12–C13	146.4(7)	149.3(10)	150.4(3)	152.2(3)
C13–C14	141.9(7)	133.2(12)	134.3(3)	150.6(4)
C14–C15	142.6(8)	150.9(11)	147.2(3)	133.5(4)
C12–C16	145.9(7)	140.4(11)	152.6(3)	141.5(3)
C13–C17	151.6(7)	150.7(11)	148.9(3)	152.4(4)
C14–C18	150.9(8)	151.5(11)	148.8(4)	149.5(4)
C16–C20	150.8(7)	140.6(9)	140.2(3)	139.7(3)

[a] Centroid C1–C5; [b] centroid C12–C16; [c] centroid C12, C16, C20; [d] centroid C15, C16, C20.

produce a dicarbonyl complex **2** with two ν(CO) bands at 1872 and 1933 cm^{-1} (hexane). The relative yields of this complex rise with increasing CO pressure: at $p(CO) \approx 1$ bar it constitutes only about 5% of the *ansa*-chromocene carbonyl product mixture; at $p(CO) \approx 5$ bar it is the only detectable product. Complex **2** is also formed when the monocarbonyl complex **1** is exposed to elevated CO pressures. Complexes **1** and **2** can be separated by crystallization from pentane or hexane.

Complex **2** crystallizes in the form of red cubes. An X-ray diffraction study (Section 4) reveals the molecular structure represented in Fig. 2, with the distances and bond angles listed in Tables 2 and 3. In the unbridged, permethylated complex $(C_5Me_5)_2Cr(CO)_2$ [14], the molecular structure of which is represented for comparison in Fig. 3, one η^5- and one η^3-coordinated

Table 3
Selected bond angles (deg)

	1	2	4	5
Cr–C21–O1	178.5(6)	176.8(7)	176.5(2)	178.9(2)
Cr–C22–O2	—	178.6(7)	178.4(3)	177.0(2)
Si1–C1–E1 [a]	152.9	152.9	172.7	152.1
Si1–C12–E2 [b]	151.9	173.7	—	174.7
X1–Cr–X2	147.4 [c]	124.3 [d]	130.4 [e]	125.5 [d]
C1–Si1–C12	91.7(2)	98.4(3)	101.50(9)	97.7(1)

[a] E1: best plane C1–C5; [b] E2: best plane C12–C16; [c] X1: centroid C1–C5, X2: centroid C12–C16; [d] X1: centroid C1–C5, X2: centroid C12, C16, C20; [e] X1: centroid C1–C5, X2: centroid C15, C16, C20.

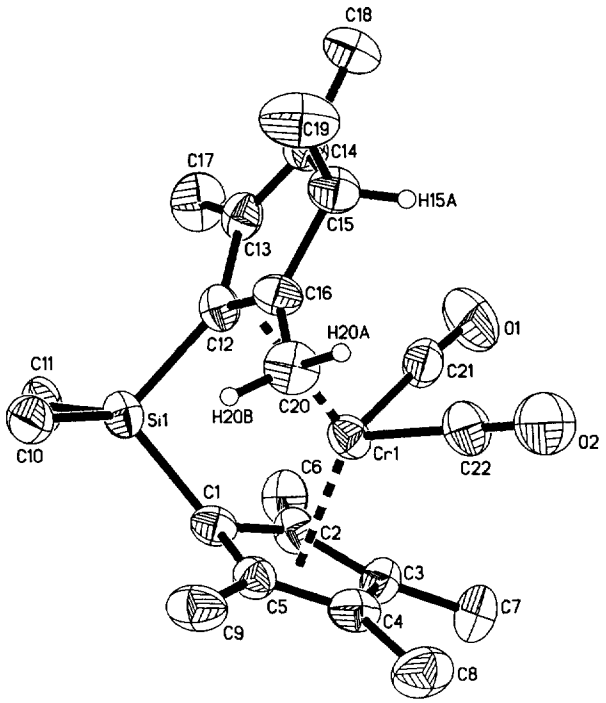

Fig. 2. Crystal structure of the dicarbonyl complex **2**. Thermal ellipsoids are drawn at the 50% probability level. Hydrogen atoms generally omitted for clarity; H15, H20a and H20b with arbitrary radii.

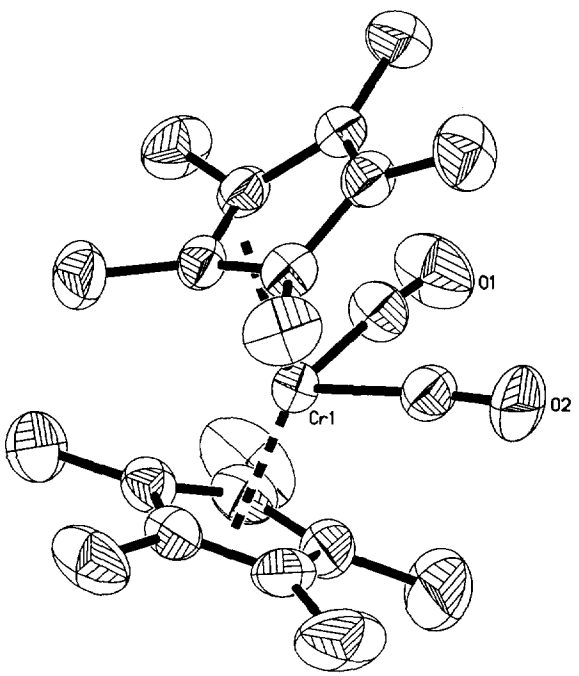

Fig. 3. Crystal structure of decamethylchromocene dicarbonyl as reported in Ref. [14]. Thermal ellipsoids are drawn at the 50% probability level. Hydrogen atoms are omitted for clarity.

C_5 ring complete the 18-electron valence shell configuration of the Cr centre. The Me_2Si-bridged dicarbonyl complex **2** on the other hand contains, besides one η^5-C_5Me_4 ligand with normal Cr–C distances of 215–225 ppm, an unusual η^3-coordinated ligand unit $C_5(H)Me_3CH_2$.

This ligand fragment is obviously derived from a C_5Me_4 unit by abstraction of a hydrogen atom from one of the α-positioned methyl groups and its transfer to the adjacent β-positioned carbon atom of the C_5 ring. The Cr centre is in bonding contact with the exocyclic α-CH_2 group and the adjacent C(α) and C(*ipso*) atoms; the Cr–C bond distances are 219–241 pm, similar to those of 215–243 pm for the endocyclic allyl fragment in $(C_5Me_5)_2Cr(CO)_2$ [14]. Cr–C distances of 330–380 pm for the remaining three C_5 ring C atoms, on the other hand, are distinctly beyond the range of bonding contacts. The asymmetric η^3-coordination of one ring affects the coordination of the other η^5-bound ring. The distance Cr–C(2) is shortened by 2 pm while the distance Cr–C(5) is 10 pm longer than in complex **1**.

In comparison to the monocarbonyl complex **1**, the bridging Si atom is located surprisingly close to the mean plane of the η^3-bound C_5 ring. In complex **2** much of the strain caused by the Si bridge appears to be removed, as indicated by an out-of-plane bending of the Si–C(12) bond by less than 7° (in the opposite direction to that in complex **1**). The Si–C(1) bond at the η^5-coordinated ring, however, still shows the same out-of-plane deviation (27°) as in complex **1**, while the Si centre, with a C(*ipso*)–Si–C(*ipso*) angle of 98.4°, is closer to tetrahedral geometry than in the monocarbonyl complex **1**.

In the ^{1}H NMR spectrum of complex **2** one observes 11 signals, all of which can be assigned by the results of a ROESY experiment (Table 4). Of the signals in the range δ 1.09–2.44 ppm, seven are due to the methyl groups at the C_5 rings, the one at δ 2.29 ppm, with an integrated intensity of only 1H, to the H atom at the sp^3-hybridised C atom in β-position of the C_5 ring. The resonances of the CH_2 group occur at δ 1.32 and 3.85 ppm. The signals of the methyl groups C(17) and C(18) which are attached to the non-coordinated C_5 ring atoms C(13) and C(14) are about twice as broad ($\nu_{1/2} \approx 5$ Hz) as those of the other methyl groups, probably due to an increased J^5-coupling in the homoallyl system C(17)–C(13)–C(14)–C(18). The inequivalence of the methyl resonances (including those of the Me_2Si bridge) and the lack of any exchange signals in a two-dimensional ROESY spectrum document that the structure represented in Fig. 2 is persistent also in solution.

We know of only three other transition metal complexes in which a C_5 ring is coordinated to the metal centre by way of an exocyclic allyl fragment when there is also an endocyclic coordination possible: the zirconium complexes $[Me_2C(\eta^5\text{-}C_5H_4)(\eta^3\text{-}C_{13}H_8)ZrCl(\mu\text{-}H)]_2$ and $[Me_2C(\eta^5\text{-}C_5H_4)(\eta^3\text{-}C_{13}H_8)ZrCl(\eta^5\text{-}C_5H_5)]_2$ [21], and the molybdenum complex $(MeS)_2C(\eta^5\text{-}C_5H_4)(\eta^3\text{-}C_5H_3C(SMe)_2)Mo(CO)_2$ [22]. In all these, two C_5 rings are connected by a single-atom bridge. This supports the notion that the release of steric strain, which would otherwise be caused by such a short bridge, is the main driving force toward formation of an exocyclic allyl structure, which allows for a less strained contact of all three ligand carbon atoms with the metal centre.

Table 4
^{1}H NMR data of the dicarbonyl complexes **2**, **3**, **4** and **5** in benzene-d_6

Chemical shift (ppm)				
2a [a]	**3b** [b]	**4a** [a]	**5** [a]	
2.44(s)	2.4(s)	1.36(s)	2.22(s)	$-CH_3$ (6)
1.79(s)	1.8(s)	1.87(s)	1.74(s)	$-CH_3$ (7)
1.78(s)	1.79(s)	1.85(s)	1.81(s)	$-CH_3$ (8)
1.28(s)	1.3(s)	2.02(s)	1.29(s)	$-CH_3$ (9)
1.96(s)	1.9(s)	1.69(s)	1.19(d) (J = 7.3 Hz)	$-CH_3$ (17)
1.63(s)	1.6(s)	1.92(s)	1.70(s)	$-CH_3$ (18)
1.09(d) (J = 7.5 Hz)	0.90(d) (J = 7.5 Hz)	1.02(s)	1.50(s)	$-CH_3$ (19)
3.85(d) (J = 2.6 Hz)	2.97(d) (J = 2.6 Hz)	1.95(d) (J = 2.6 Hz)	3.68(d) (J = 2.4 Hz)	$=CH_2$ (20a)
1.32(d) (J = 2.6 Hz)	1.3(d) (J = 2.6 Hz)	3.32(d) (J = 2.6 Hz)	1.04(d) (J = 2.4 Hz)	$=CH_2$ (20b)
−0.26(s)	-0.22(s)	0.32(s)	−0.17(s)	Si–CH_3 (10)
0.54(s)	0.54(s)	0.02(s)	0.52(s)	Si–CH_3 (11)
2.29(q) ($J \approx 7$ Hz)	3.72(m)	3.44(bs)	2.96(q) ($J \approx 7$ Hz)	–C(H)CH_3

[a] Assignment by 2D-ROESY spectrum.
[b] Not isolated, assignment by comparison with **4**.

2.3. *Kinetics of the reaction* **1** + CO → **2**

In the formation of the exocyclic allyl unit of complex **2**, a haptotropic shift of the metal centre is combined with the shift of a proton from an α-CH_3 group to a β-C atom of the C_5 ring. While there is ample precedent for the intramolecular shift of a proton from a CH_3 substituent to the metal centre, under formation of 'tuck-in' structures [23], as well as for metal-mediated proton shifts between alternative ligand positions [24], these processes generally require an open coordination site. Neither in the monocarbonyl complex **1** nor in a putative, unrearranged dicarbonyl intermediate $Me_2Si(C_5Me_4)_2Cr(CO)_2$, does a coordinatively unsaturated metal centre appear to be present however.

In the hope of gaining insights into the course of this reaction, we have undertaken a study of its kinetics. The rate of the reaction **1** + CO → **2** was followed in an IR cell suitable for measurements under variable CO pressures and temperatures [25,26]. The data thus obtained

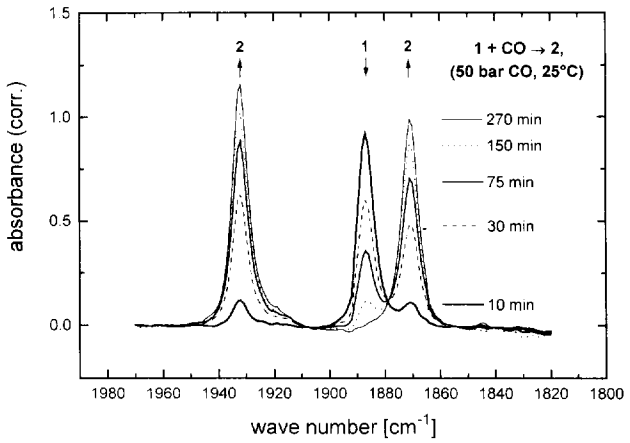

Fig. 4. IR spectra for the reaction of **1** to **2** in the presence of 50 bar CO at 25 °C in methylcyclohexane solution, after baseline correction and subtraction of the solvent spectrum.

do not indicate the appearance of a reaction intermediate; an isosbestic point at 1878 cm^{-1} (Fig. 4) can be taken as evidence that the concentration of any intermediates remains quite small.

The reaction follows a simple second-order rate law, first-order in complex **1** and first-order in CO. The rate constants thus determined (Table 5) are lower by about one order of magnitude than those obtained at the same temperatures for the related reaction $(C_5H_5)_2Cr(CO) + CO \rightleftharpoons (C_5H_5)_2Cr(CO)_2$ or those estimated for the reaction $Me_4C_2(C_5H_5)_2Cr(CO) + CO \rightleftharpoons Me_4C_2(C_5H_5)_2Cr(CO)_2$ [13]. This retardation appears to be a consequence of ligand permethylation. Similar retardation effects have been observed also for the substitution of CO by phosphine or phosphite ligands in $C_5Me_5Rh(CO)_2$ relative to $C_5H_5Rh(CO)_2$ [27].

The data in Table 5 yield an activation enthalpy of $H^{\neq} = 51 \pm 3$ kJ mol^{-1} and an activation entropy of $S^{\neq} = -136 \pm 10$ J mol^{-1} K^{-1}. Similar values have been reported for activation parameters of related reactions [13,27], for which the rate-determining step is assumed to be an associative attack by the new ligand (Table 6), such as the substitution reactions of $C_5H_5Rh(CO)_2$ or $C_5Me_5Rh(CO)_2$, studied by Basolo and coworkers [27].

Conduction of the reaction **1** + CO → **2** in benzene-d_6 did not lead to any detectable incorporation of deuterium into complex **2**. Addition of $[FeCp_2][PF_6]$ (10 mol.%) as an oxidant or of $LiAl(O^tBu)_3H$ as a reductant did not have any noticeable effect on the rate

Table 5
Second-order rate constants for reaction **1** + CO → **2** in methylcyclohexane

Temperature (K)	k_p (10^{-7} s^{-1} bar^{-1})	k_c [a] (10^{-5} l mol^{-1} s^{-1})
263	3.28 [b]	3.41 [b]
273	8.1 ± 1.7 [c]	8.4 ± 1.7 [c]
298	48 ± 1 [d]	50 ± 1 [d]
308	114 ± 15 [c]	118 ± 16 [c]

[a] $c(CO) = 9.6 \times 10^{-3}$ mol l^{-1} bar^{-1} $p(CO)$, Ref. [26], determined from measurements at: [b] 10 bar CO, [c] 5 and 10 bar CO and [d] 5, 10, 20, 30, 40 and 50 bar CO.

of formation of complex **2**. An electron-transfer catalysis similar to that found to accelerate the formation of $Me_4C_2(C_5H_4)_2Cr(CO)_2$ [13] is thus unlikely to be operative in this case.

In the absence of truly distinctive data, further remarks on possible mechanisms for the reaction **1** + CO → **2** must remain tentative. Nevertheless, the stability of complex **1** against loss of CO, even under sublimation conditions, as well as the activation parameters given in Table 6, would indicate that an associative reaction of complex **1** with CO is the initial, rate-determining step of this reaction sequence. A resulting dicarbonyl intermediate $Me_2Si(\eta^5\text{-}C_5Me_4)(\eta^3\text{-}C_5Me_4)_2Cr(CO)_2$, comparable to the unbridged dicarbonyl $(\eta^5\text{-}C_5Me_4)(\eta^3\text{-}C_5Me_4)Cr(CO)_2$ [14], would then have to rearrange to complex **2** by a shift of a hydrogen atom.

If we exclude that this hydrogen shift occurs in a direct, concerted manner (vide infra), an open coordination site would be required for a metal-mediated hydrogen shift. Easiest to reach from the η^3-haptomer would undoubtedly be the coordinatively unsaturated species $Me_2Si(\eta^5\text{-}C_5Me_4)(\eta^1\text{-}C_5Me_4)Cr(CO)_2$, since its formation would be aided by a substantial release of steric strain. Once an open coordination site is available, the shift of a H atom from a CH_3 group to the chromium centre and from there to a C atom in β-position of the C_5 ring can be assumed to be fast in comparison with the overall reaction rate. Related hydrogen shift reactions in methyl-substituted chromium allyl complexes have been observed by Kreiter and coworkers to be fast [24]. Altogether, the reaction path represented in Scheme 1 appears to be in reasonable accord with the available data.

Table 6
Activation parameters for **1** + CO → **2** and for related reactions

	Addition of CO to		Substitution of CO by phosphanes or phospites	
	1	$Cp_2Cr(CO)$ [a]	$(C_5Me_5)Rh(CO)_2$ [b]	$CpRh(CO)_2$ [b]
$\Delta H^{\neq}$ (kJ mol^{-1})	51 ± 3	58 ± 6	≈ 60	60–75
$\Delta S^{\neq}$ (J mol^{-1} K^{-1})	−136 ± 10	−89 ± 15	≈ −150	≈ −80

[a] Ref. [13]; [b] Ref. [27].

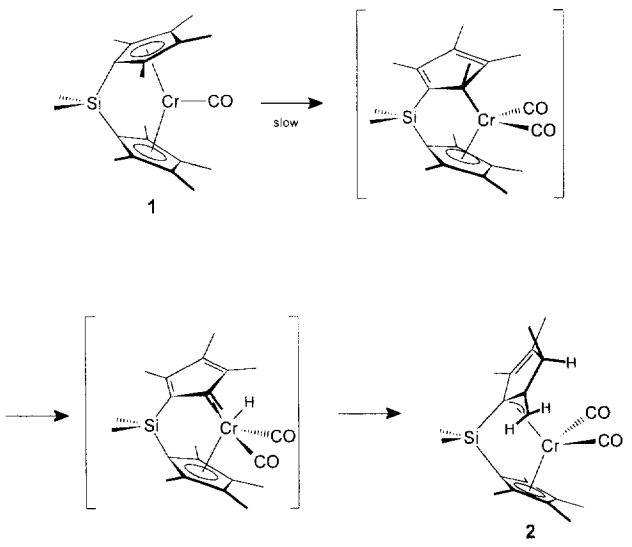

2.4. *Further rearrangements of complex 2*

Whereas the monocarbonyl complex **1** is remarkably stable against thermolysis (no changes in the ^{1}H NMR spectrum after 10 days in toluene-d_8 at 60 °C), this is not the case for **2**. Under these conditions, **2** dissociates partly to **1** (approximately 10%) while isomerizing mainly to the tautomeric complex **4**. In distinction to **2** the ^{1}H NMR spectrum of **4** (Table 4) contains neither the quartet of a proton at the C_5 ring nor the doublet of the methyl group coupled to it. Instead one observes an additional singlet with an integrated intensity of 3H and a broad singlet with an intensity of 1H. From these, and the persistent asymmetry of the complex, we conclude that another H-shift has taken place, in this case to the *ipso*-C atom of the C_5 ring (C(12)). A two-dimensional ROESY experiment confirms this assumption by showing the spatial neighbourhood of the single proton to a methyl group at the silicon centre (C(10)) and to an α-methyl group (C(17)). The two methyl groups at the non-coordinated carbon atoms (C(17) and C(18)) interchange with respect to their chemical shifts compared to the spectrum of **2**, as expected from the interchange of their α- or β-position relative to the sp^3-centre, which is associated with the proposed H-shift.

An EI mass spectrum, identical to that of **2**, with the parent peak M^+ at $m/e = 406$ and the base peak $[M - 2CO]^+$ at $m/e = 350$, further indicates that **4** is a tautomer to **2**. The ν(CO) bands at 1855 cm^{-1} and 1918 cm^{-1} are shifted by 14–16 cm^{-1} to lower wavenumbers. Crystals suitable for an X-ray diffraction study have been obtained by slow evaporation of the solvent from a pentane solution at −20 °C. The structure shown in Fig. 5 is in agreement with the conclusions from the two-dimensional ROESY experiment. As required by the coordination of the allyl fragment to the chromium centre, the hydrogen atom at the *ipso*-position is found on the *exo*-site of the ring. The Cr–C distances and Cr–centroid distances are comparable with those of complex **2**. The coordination of the allylic fragment C15, C16, C20 results in an out-of-plane bending of the methyl group C19 of 30° and in a rotation of the CH_2 group around the C16–C20 bond of 25°. The introduction of an sp^3-centre at the bridgehead position reduces the steric strain at the silicon bridge. The Si–C1 bond deviates only by 7° from the mean plane of the η^5-coordinated ring (27° in complex **2**). In addition, the two Cr–(α) distances are more even here than in complex **2**.

During the thermal isomerization of **2**, a side- or by-product **3** was observed, which disappeared again in the course of the reaction. The ^{1}H NMR spectrum of **3** is very similar to that of **2** (Table 4). Only the proton at the sp^3-centre, C(15), the methyl group at the same centre, C(19), and the proton of the CH_2 group oriented in the direction of the sp^3-centre, H(20b), show significant differences in their chemical shifts. For all other signals – especially for those of the η^5-coordinated ring – changes relative to those of **2** remain small, in general smaller than the NMR linewidth. The change of the chemical shifts of the two substituents at the sp^3-centre in opposite directions, with the rest of the ligand framework remaining in place, is explained by a rotation of the η^3-coordinated ring about the Si–C(*ipso*) bond, which would transfer the hydrogen at C(15) into an *exo*-position. Such a structure for **3** (Scheme 2) is in agreement with the changes observed in the NMR spectrum and with the mechanism of the isomerization to be proposed later on.

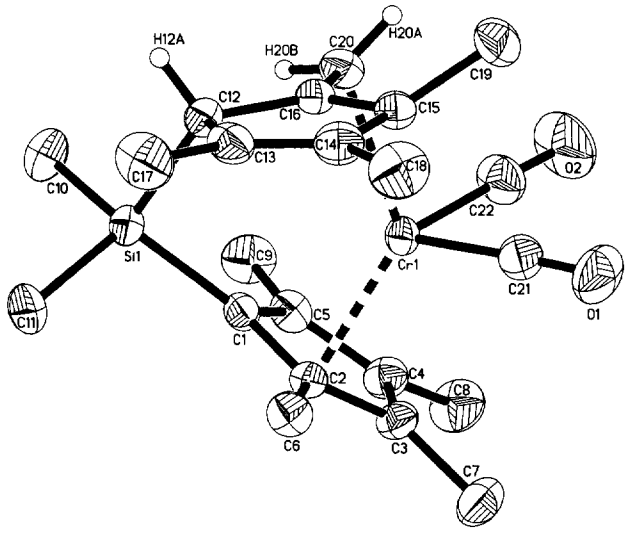

Fig. 5. Crystal structure of the dicarbonyl complex **4**. Thermal ellipsoids are drawn at the 50% probability level. Hydrogen atoms generally omitted for clarity; H12a, H20a and H20b with arbitrary radii.

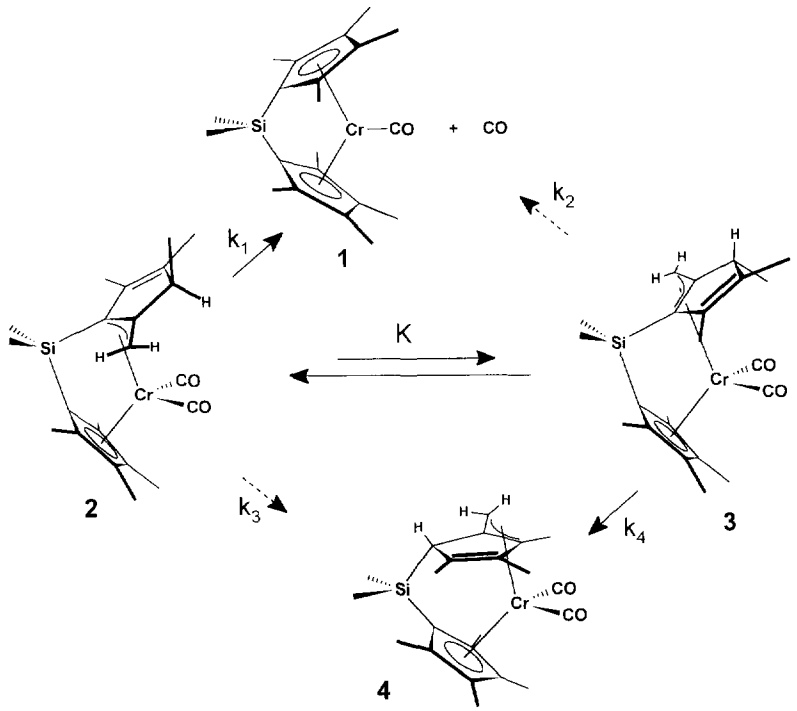

Scheme 2.

The tautomeric product **4** when heated in toluene for several days at temperatures of 70 °C or above equilibrates with a further tautomer **5**. The ^{1}H NMR spectrum of the latter (Table 4) indicates that a C_1-symmetric geometry is again sustained. The doublet of a coupled methyl group reappearing at 1.18 ppm and the corresponding quartet for the proton at 2.95 ppm indicate a migration of the hydrogen away from the bridgehead carbon.

Crystallization in hexane at −30 °C afforded red crystals of **5** suitable for an X-ray diffraction study. In the crystal structure obtained (Fig. 6), the hydrogen is found in an *endo*-position at the α-C atom (C(13)). Excluding the three non-coordinated carbon atoms (C(13)–C(15)), the structure of complex **5** is almost identical with that of the 3-*endo*-tautomer **2**, as shown by the superposition of the two structures shown in Fig. 7.

2.5. *Kinetics and mechanisms of the rearrangement* $2 \rightarrow 3 \rightarrow 4$

The kinetics of the thermal rearrangement were determined by NMR spectroscopy. The concentration profiles of all participating complexes are independent of the starting concentration of **2**. This indicates that only first-order reactions take place, as expected for intramolecular rearrangements. **2** and **3** show a constant ratio of their concentrations after an induction period of approximately half an hour (Fig. 8). This is to be expected if the equilibrium $\mathbf{2} \rightleftharpoons \mathbf{3}$ is fast compared to the formation of **4** and **1**. After such an equilibrium has been reached, the formation of **4** and **1** and the disappearance of **2** and **3** take place according to a first-order rate law (Figs. 8 and 9). The velocity of the formation

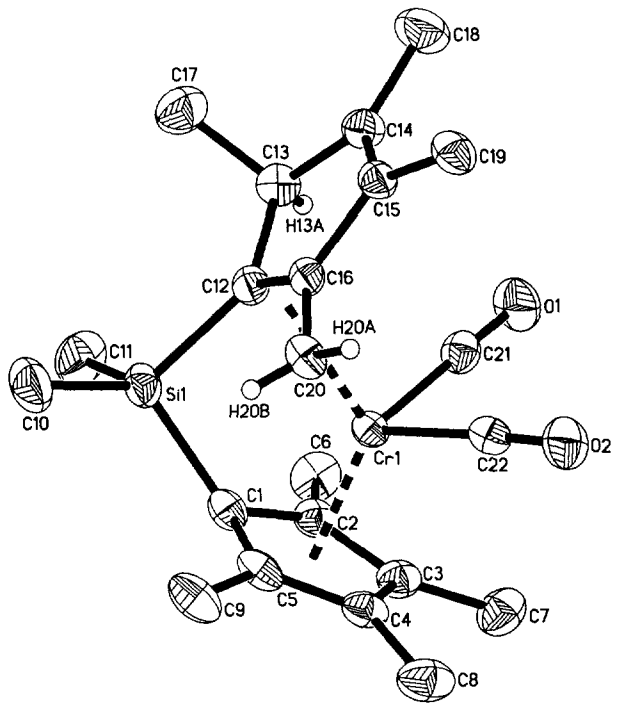

Fig. 6. Crystal structure of the dicarbonyl complex **5**. Thermal ellipsoids are drawn at the 50% probability level. Hydrogen atoms generally omitted for clarity; H13, H20a and H20b with arbitrary radii.

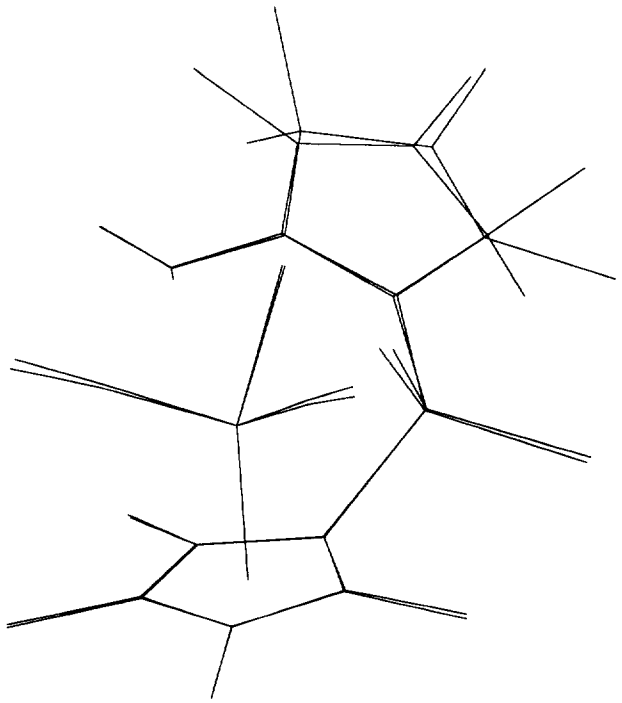

Fig. 7. Superposition of the crystal structures of **2** and **5** as wire models.

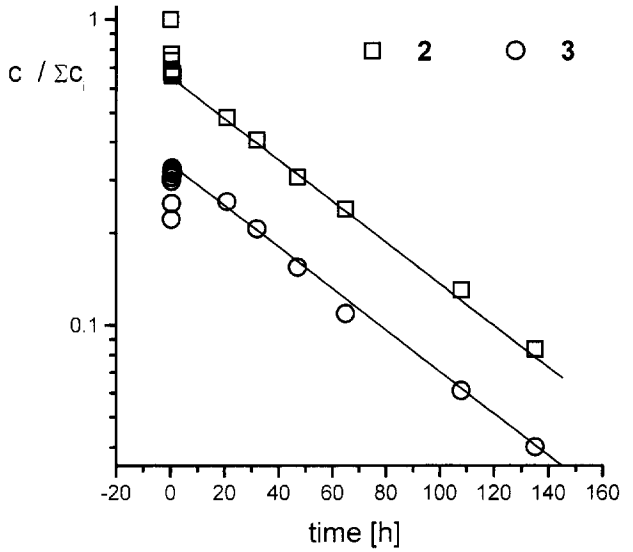

Fig. 8. Concentrations of **2** and **3** during the isomerization to **4** (half-logarithmic scale), with fast initial concentration changes and parallel regression lines at $t > 10$ h, indicating a fast equilibrium followed by a first-order reaction.

of the monocarbonyl complex **1** decreases with time in a manner compatible with its formation from **2**. Based on these observations we propose the reaction path represented in Scheme 2 for the rearrangement of **2** to **4**.

Assuming that the equilibrium **2** ⇌ **3** is fast compared to the other reactions, we were able to extract rate and equilibrium constants in toluene-d_8 at 55 °C from the experimental data. These parameters are represented in Table 7, the calculated concentration profiles together with the experimental data in Fig. 9. Only concentrations at $t > 30$ min were used for the determination of

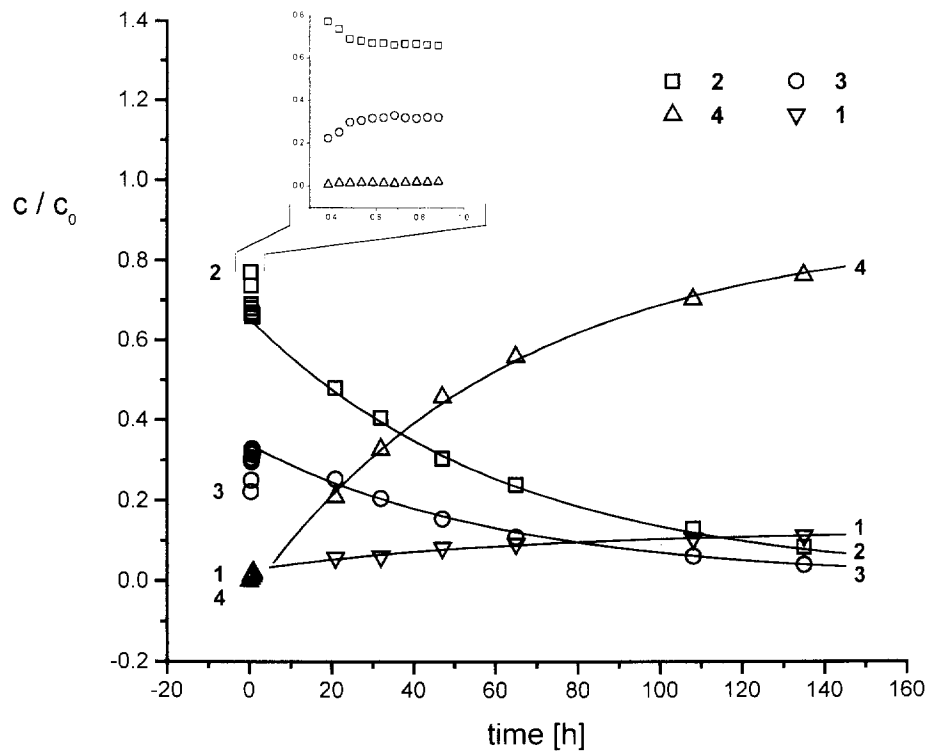

Fig. 9. Concentrations of reaction participants in the isomerization of **2** to **4** and the interpolation graphs for first-order reactions, calculated with the assumption of a fast equilibrium **2** ⇌ **3**.

Table 7
Rate and equilibrium constants for the thermal rearrangement **2** ⇌ **3** → **4**

T (K)	$K = [3]/[2]$	$k' = k_1 + Kk_2\ s^{-1}$	$k'' = k_3 + Kk_4\ s^{-1}$
328	0.54	5.3×10^{-7}	3.6×10^{-6}
343	0.5	1.4×10^{-5}	3.1×10^{-5}

the rate constants, since the induction period is dominated by the fast equilibrium **2** ⇌ **3**. The much greater velocity of the equilibrium reaction prevented a determination of the rate constants k_1–k_4 per se; only the mixed rate constants $k' = k_1 + Kk_2$ and $k'' = k_3 + Kk_4$ can be obtained. It was not possible to decide, therefore, whether **4** is formed directly from **2** or via **3** as a necessary intermediate. An initial lag phase, which gives rise to an interpolation graph with an apparent negative concentration at $t = 0$, indicates that **4** originates predominantly from **3** rather than from **2**. An analogous argument with regard to an apparent positive concentration of **1** at $t = 0$ leads to the conclusion that the dissociation to **1** originates mainly from **2**. Although the deviations of the apparent initial concentrations of **1** and **4** from zero are close to the error margin, we propose reaction Scheme 2, i.e. the formation of **1** from **2** and of **4** from **3** in plausible accord with mechanistic considerations to be discussed below.

Compared with the reaction **1** + CO → **2**, the rearrangement of the latter is slow. At 35 °C and 5 bar CO, the lowest CO pressure used, the formation of **2** is faster by an order of magnitude than its rearrangement to **4** at 55 °C. The dissociation to the monocarbonyl complex **1** is slower by another order of magnitude. This explains why none of these reactions are observed during the kinetic studies on the formation of the dicarbonyl complex **2**.

If the isomerization is carried out at higher temperatures, the kinetic parameters obtained are less reliable due to thermal decomposition reactions of products and reactants. Nevertheless, we estimate from the rate and equilibrium constants obtained at 70 °C (Table 7) activation parameters of 130 kJ mol^{-1} and $\Delta S^{\neq} \approx$ 50 J mol^{-1} K^{-1} for the rearrangement to **4** and of $\Delta H^{\neq}$ ≈ 200 kJ mol^{-1} and $\Delta S^{\neq} \approx$ 250 J mol^{-1} K^{-1} for the dissociation to the monocarbonyl complex **1**.

For an intramolecular rearrangement of **2** to **4** a direct *antara*-facial shift of the hydrogen appears impossible for steric reasons. Hydrogen transfer to and from the solvent is also excluded, because no deuterium incorporation was observed when deuterated solvents (C_6D_6, toluene-d_8) were used. The most probable possibility for the hydrogen to arrive in an *exo*-position (which is required to retain the allyl fragment in coordination to the chromium) is a rotation of the η^3-coordinated ring about the Si–C(*ipso*) bond. This rotation could proceed through a transition state, which contains one of the C_5 ring units η^1-coordinated through the exocyclic CH_2 group (Fig. 10). Such a rotation would lead to complex **3**, a subsequent *supra*-facial [1,3] H-shift to **4**. The fast interconversion between **2** and **3** indicates that a transition state of this type is rather easily accessible. According to this mechanism, **3** is a necessary intermediate for the rearrangement of **2** to **4** such that $k_1 = 0$ and $k' = Kk_2$ (Scheme 2). As discussed above, the kinetic data are compatible with this notion.

The absence of a direct dissociation of **4** to the monocarbonyl complex **1** appears to be a consequence of **4** having its hydrogen atom in an *exo*-position at the C_5 ring. The metal centre would thus participate in the C–H activation during formation of **2** as well as in its reverse during regeneration of **1**. Similar arguments lead to the conclusion that the dissociation to the monocarbonyl complex **1** is unlikely to occur from **3**. Accordingly, we have to assume that $k_4 = 0$ (Scheme 2).

2.6. *Rearrangement of 4 to 5*

At temperatures of 70 °C, where the isomerization of **4** to **5** can be observed within reasonable times, decomposition becomes a major problem, such that reliable rate constants could not be determined. At 70 °C in toluene-d_8, an equilibrium between **4** and **5** is reached after ca. 14 days with $t_{1/2} \approx$ 1.5–2 days (Fig. 11), when the reaction is started either with **4** (obtained in situ by isomerization of **2**) or with **5**. Under these conditions we find an apparent equilibrium constant $K = [5]/[4] =$ 1.7.

During the isomerization of **4** to **5**, some additional small signals indicate the formation of still another isomer **6**, probably in equilibrium with **5**. Its concentration is so low (maximally 6%) that only a few of its

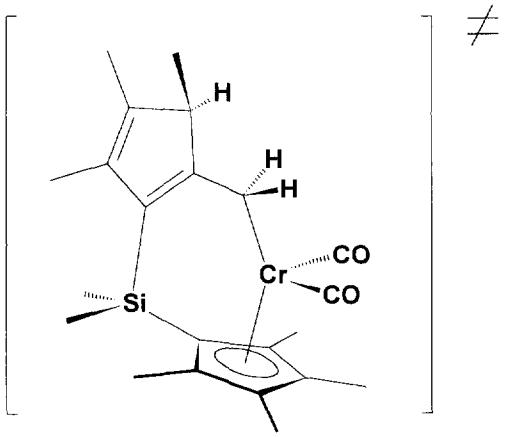

Fig. 10. Transition state postulated for the interconversion of **2** and **3** by rotation of the η^3-coordinated ring around the Si–C(*ipso*) bond.

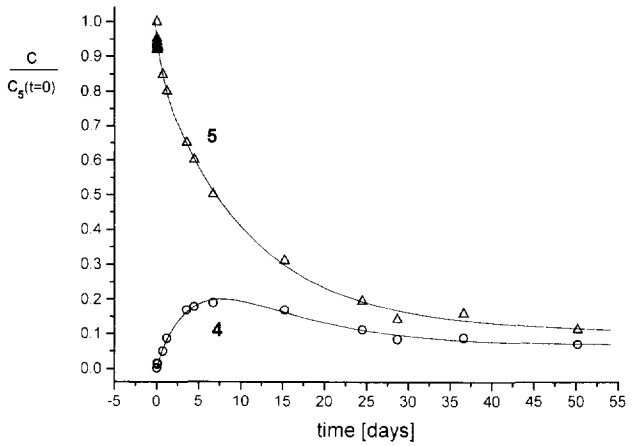

Fig. 11. Concentrations of tautomers **4** and **5** during the isomerization started with **5**.

NMR signals are distinguishable from those of the other tautomers. We would assume that this compound is the 5-*exo*-H-tautomer of **5**. Its rapid formation and subsequent constant ratio to the concentration of **5** are similar to the equilibrium observed between **2** and **3**. As expected from the steric strain caused by a methyl group in an *endo*-α position, the equilibrium constant $K = [\mathbf{6}]/[\mathbf{5}] \approx 1/15$ is much smaller than that ($K \approx 1/2$) observed for **2** ⇌ **3**.

In analogy to the rearrangement of **2** to **4**, the formation of **5** from **4** requires a hydrogen migration as well as a ring rotation reaction. We propose Scheme 3 as a summary of the observed isomerization reactions of the complexes **2** to **6**. Hydrogen migrations can occur either on the *endo*- or on the *exo*-side of the C_5 ring. The *endo*- and *exo*-isomers are interconverted by comparatively fast reversible flips of the η^3-coordinated ring. Small amounts of **2** (less then 1%, too small for quantitative determination) were observed when the isomerization of **5** to **4** was started with pure **5**. This indicates that hydrogen migrations along at least one of the paths connecting **2** with **5** are also reversible, as are those connecting **4** with **5**. Our data do not exclude any

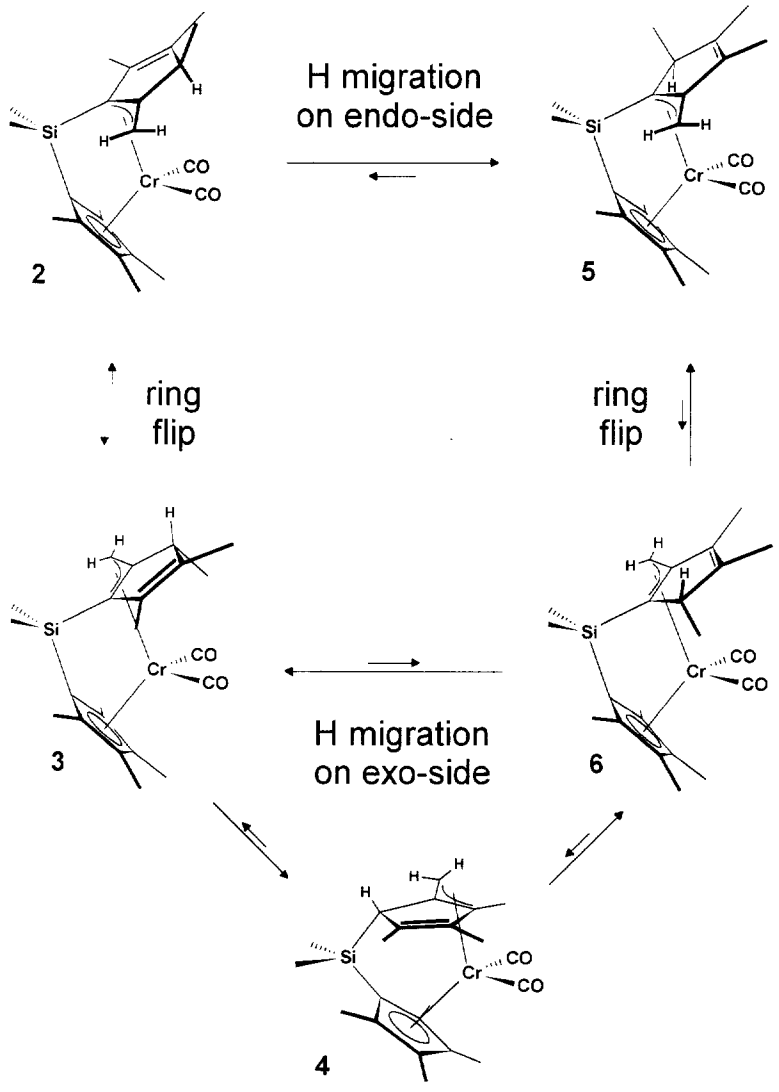

Scheme 3.

one of the alternative reaction paths as a main contributor to the observed isomerizations.

3. Conclusions

The observations reported above demonstrate that cyclopentadienyl ligands do not always conform with their generally perceived role of inert ligands. In addition to the intramolecular C–H activation and hydrogen migration reactions observed here and in other cases [23,24], we find it particularly remarkable with what ease an exocyclic allyl coordination allows the permethylated cyclopentadienyl unit to flip from one of its π-sides to the other. Ligand mobility of this kind might play a greater role than hitherto assumed also for the stereochemistry of other C_2-symmetric *ansa*-metallocene complexes, e.g. in homogenous catalysis reactions.

4. Experimental

4.1. General information

All operations were carried out under exclusion of air and moisture, using Schlenk and vacuum line techniques. Solvents used were dried by standard methods, degassed and stored under argon. NMR spectra were obtained by use of a Bruker WM 250 (250.13 MHz, room temperature) spectrometer. For ROESY experiments a Bruker DRX 600 (600.13 MHz, 300 K) was used (internal standard δ (C_6D_5H) 7.15 ppm or δ ($C_6D_6CD_2H$) 2.03 ppm). IR spectra were measured on a Matson FT-IR Polaris spectrometer, C/H elemental analyses on a Leybold Heraeus CHN analyser and mass spectra on a Varian MAT 112 S/312.

Anhydrous $CrCl_2 \cdot x$THF ($x = 1.7$) was obtained from Cr metal and HCl/THF [28] or by reduction of $CrCl_3 \cdot 3$THF with $LiAlH_4$ [29].

4.2. $Me_2Si(C_5Me_4)_2Li_2$

The ligand was prepared by a variation of a method published by Jutzi and coworkers [15] and Marks and coworkers [16]. After the condensation of pentan(3)one with two equivalents of acetic aldehyde in a basic medium, the desired product, γ-pyrone, was separated from the reaction mixture by steam distillation; this procedure proved to be more effective than separating the layers in a separation funnel by aid of an acid [30]. Dehydration of the γ-pyrone to tetramethylcyclopentenone was performed as described in the literature [30]. Reduction of tetramethylcyclopentenone and the dehydration of the intermediate alcohol to $C_5Me_4H_2$ was done as a one-pot synthesis following a method published by Schmitt and Özmann [31]. The introduction of the dimethylsilyl bridge and the lithiation was carried out as described in the literature [15,16].

4.3. $Me_2Si(C_6Me_4)_2Cr(CO)$ (1)

To 2.41 g (7.7 mmol) $Me_2Si(C_5Me_4)_2Li_2$ in 100 ml THF was added 1.55 g $CrCl_2 \cdot x$THF in small portions over a period of 1.5 h at room temperature under a CO atmosphere. The brown solution was subsequently stirred under CO for 3 h. The solvent was removed and the solid extracted with pentane until the filtrate remained colourless. The extract was concentrated to ca. 10 ml and placed in a refrigerator at −70 °C overnight. One obtains 1.14 g (3.0 mmol, 39%) of $Me_2Si(C_5Me_4)_2Cr(CO)$ as red–brown crystals. ^{1}H NMR (C_6D_6, δ in ppm): 1.72 (s, 12H, $-CH_3$), 1.64 (s, 12H, $-CH_3$), 0.48 (s, 6H, Si–CH_3). IR: ν(CO) 1888 cm^{-1} (hexane); 1876 cm^{-1} (toluene). MS (170 °C, EI): 378 (M^+), 350 ($M^+ - CO$). Anal. Found: C, 66.75; H, 8.15. $C_{21}H_{30}CrSiO$ (378.55) Calc.: C, 66.63; H, 7.99%.

4.4. $Me_2Si(C_5Me_4)(C_5(3\text{-}H)(2\text{-}CH_2)Me_3)Cr(CO)_2$ (2)

200 mg (0.53 mmol) $Me_2Si(C_5Me_4)_2Cr(CO)$ in 20 ml pentane was transferred to a laboratory autoclave under exclusion of air and stirred for 24 h under 50 bar of CO. The deep red solution thus obtained was freed from insoluble black by-products by filtration and concentrated to 10 ml. After 3 days at −30 °C, 150 mg $Me_2Si(C_5Me_4)_2Cr(CO)_2$ (0.37 mmol, 70%) was obtained as deep red, finely crystalline powder. ^{1}H NMR (C_6D_6, δ in ppm): 3.85 (d, 1H, $J = 2.6$ Hz), 2.44 (s, 3H), 2.29 (q, 1H, $J \approx 7$ Hz), 1.96 (s, 3H), 1.79 (s, 3H), 1.78 (s, 3H), 1.63 (s, 3H), 1.32 (d, 1H, $J = 2.6$ Hz), 1.28 (s, 3H), 1.09 (d, 3H, $J = 7.5$ Hz), 0.54 (s, 3H), −0.26 (s, 3H). IR: ν(CO) 1858, 1924 cm^{-1} (toluene); 1874, 1918 cm^{-1} (Nujol). MS (170 °C, EI): 406 (M^+), 378 ($M^+ - CO$), 350 ($M^+ - 2CO$). Anal. Found: C, 65.40; H, 7.57. $C_{22}H_{30}CrSiO_2$ (406.55) Calc.: C, 64.99; H, 7.44%.

4.5. $Me_2Si(\eta^5\text{-}C_5Me_4)(\eta^3\text{-}C_5(1\text{-}H)(2\text{-}CH_2)Me_3)Cr(CO)_2$ (4)

70 mg (0.17 mmol) **2** was dissolved in 10 ml toluene under exclusion of air and heated for 22 h to 70 °C. The solvent was removed in vacuo and the residue dissolved in 10 ml pentane. The solution was decanted from insoluble by-products and concentrated. By crystallization at −20 °C, 21 mg (0.05 mmol, 31%) of complex **4** was obtained in the form of black crystals. ^{1}H NMR (C_6D_6, δ in ppm): 3.44 (bs, 1H), 3.32 (d, 1H, $J = 2.6$ Hz), 2.02 (s, 3H), 1.95 (d, 1H, $J = 2.6$ Hz), 1.92 (s, 3H), 1.87 (s, 3H), 1.85 (s, 3H), 1.69 (s, 3H), 1.36 (s, 3H), 1.02 (s, 3H), 0.32 (s, 3H), 0.02 (s, 3H). IR: ν(CO) 1855,

1918 cm^{-1} (methylcyclohexane); 1845, 1910 cm^{-1} (toluene). MS (RT, EI): 406 (M^+), 350 ($M^+ - 2CO$), 175 ($M^{2+} - 2CO$). Anal. Found: C, 65.21; H, 7.60. $C_{22}H_{30}CrSiO_2$ (406.55) Calc.: C, 64.99; H, 7.44%.

4.6. $Me_2Si(\eta^5\text{-}C_5Me_4)(\eta^3\text{-}C_5(5(endo)\text{-}H)(2\text{-}CH_2)Me_3)Cr(CO)_2$ (5)

170 mg (0.41 mmol) **2** in 20 ml toluene was stirred for 8 days at 90 °C. The solution was freed of insoluble by-products by filtration and the solvent removed in vacuo. Crystallization of the remaining brown solid from 8 ml pentane at −30 °C gave compound **5** as red crystals (59 mg, 0.15 mmol, 35%). ^1H NMR (C_6D_6, δ in ppm): 3.68 (d, 1H, $J = 2.4$ Hz), 2.96 (q, 1H, $J \approx 7$ Hz), 2.22 (s, 3H), 1.81 (s, 3H), 1.74 (s, 3H), 1.70 (s, 3H), 1.50 (s, 3H), 1.29 (s, 3H), 1.19 (d, 3H, $J = 7.3$ Hz), 1.04 (d, 1H, $J = 2.4$ Hz), 0.52 (s, 3H), −0.17 (s, 3H). IR: ν(CO) 1926, 1861 cm^{-1} (toluene). Anal. Found: C, 64.62; H, 7.47. $C_{22}H_{30}CrSiO_2$ (406.55) Calc.: C, 64.99; H, 7.44%.

4.7. Kinetics of the reaction from 1 to 2

A 3.25×10^{-2} M solution of **1** was reacted with CO in an IR high-pressure cell, equipped with an internal stirrer, which permits the examination of the reaction by IR spectroscopy under isothermic and isobaric conditions. Variations in the concentrations of **1** and **2** were determined by the extinction of their ν(CO) bands (for technical details see Ref. [25]).

4.8. Kinetics of the rearrangement 2 → 3 → 4 → 5

The thermal rearrangement was carried out at 55 ± 3 °C in toluene-d_8 in melt-sealed NMR tubes. For long-term experiments, ^1H NMR spectra were recorded after cooling to room temperature; the periods of ca. 15 min at room temperature were neglected for the kinetic analysis. Data points with $t < 10$ h were obtained in different sets of experiments, following the reaction directly in the spectrometer. Concentrations were obtained by integration of selected well-separated peaks. Rearrangements at higher temperatures were followed in an analogous manner; here, decomposition to NMR-silent products became a major problem, as determined by comparison with an internal ferrocene standard.

4.9. Crystal structure determinations

Data for complex **1**, **2**, **4** and **5** were collected by using a Siemens R3m/V diffractometer and Mo Kα radiation ($\lambda = 0.71073$ Å).

4.9.1. Complex 1

Crystal size (mm^3): 0.3 × 0.3 × 0.3. Crystal data: monoclinic space group $P2_1/n$, $a = 13.257(7)$ Å, $b = 10.186(5)$ Å, $c = 14.739(7)$ Å, $\beta = 90.89(4)°$, $Z = 4$, $V = 1990.1(17)$ $Å^3$, D(calc.) = 1.263 g cm^{-3}, $\mu = 0.624$ mm^{-1}, $F(000) = 808$. A total of 4354 reflections was collected, of which 3923 were independent and 3353 were used ($F > 5.0\sigma(F)$). The structure was solved by direct methods and refined by least-squares methods with the SHELXTL PLUS program package [32]. All non-hydrogen atoms were refined anisotropically. The positions of the hydrogen atoms were calculated with fixed isotropic U using the riding model technique. The final agreement factors were $R_1 = 6.67\%$ and $R_w = 7.21\%$ (unit weights).

4.9.2. Complex 2

Crystal size (mm^3): 0.2 × 0.2 × 0.2. Crystal data: orthorhombic space group $Pbca$, $a = 8.699(3)$ Å, $b = 14.713(6)$ Å, $c = 32.801(14)$ Å, $Z = 8$, $V = 4198(3)$ $Å^3$, D(calc.) = 1.286 g cm^{-3}, $\mu = 0.599$ mm^{-1}, $F(000) = 1728$. A total of 5417 reflections was collected, of which 2733 were independent and 1517 were used ($F > 4.0\sigma(F)$). The structure was solved by direct methods and refined by least-squares methods with the SHELXTL PLUS program package [32]. All non-hydrogen atoms were refined anisotropically. The positions of the hydrogens were calculated with fixed isotropic U using the riding model technique. The final agreement factors were $R_1 = 5.98\%$ and $R_w = 4.66\%$ ($w^{-1} = \sigma^2(F) + 0.0001F^2$).

4.9.3. Complex 4

Crystal size (mm^3): 0.4 × 0.3 × 0.3. Crystal data: monoclinic space group $P2_1$, $a = 949.7(2)$ pm, $b = 989.5(3)$ pm, $c = 1137.1(2)$ pm, $\beta = 103.919(8)°$, $Z = 2$, $V = 1.0371(4)$ nm^3, D(calc.) = 1.302 g cm^{-3}, $\mu = 0.622$ mm^{-1}, $F(000) = 432$. A total of 4631 reflections was collected, of which 4320 were independent and 4116 were used ($F > 2.0\sigma(I)$). The structure was solved by direct methods and refined by least-squares methods against F^2 with the SHELXL-93 program package [32]. All non-hydrogen atoms were refined anisotropically. The hydrogen atoms were found in the difference Fourier map and refined with isotropic U and idealized tetrahedral geometry for the methyl groups. The final agreement factors were $R_1 = 2.90\%$ and $R_w(F^2) = 7.35\%$ ($w^{-1} = \sigma^2(F_o^2) + (0.0438P)^2 + 0.1233P$, where $P = (F_o^2 + 2F_c^2)/3$). The absolute structure was determined with a Flack x parameter of 0.001(15).

4.9.4. Complex 5

Crystal size (mm^3): 0.2 × 0.2 × 0.2. Crystal data: monoclinic space group $P2_1/c$, $a = 1655.5(4)$ pm, $b = 1303.6(3)$ pm, $c = 1004.4(2)$ pm, $\beta = 107.45(1)°$, $Z = 4$, $V = 2.0678(8)$ nm^3, D(calc.) = 1.306 g cm^{-3}, $\mu = 0.624$ mm^{-1}, $F(000) = 864$. A total of 4993 reflections was collected, of which 4515 were independent and

3488 were used ($F > 2.0\sigma(I)$). The structure was solved by direct methods and refined by least-squares methods against F^2 with the SHELXL-93 program package [32]. All non-hydrogen atoms were refined anisotropically. The positions of the hydrogen atoms were calculated with fixed isotropic U using the riding model technique, with the exception of the hydrogen atoms H14a, H20a and H20b, which were found in the difference Fourier map and refined isotropically. The final agreement factors were $R_1 = 4.39\%$ and $R_w(F^2) = 10.67\%$ ($w^{-1} = \sigma^2(F_o^2) + (0.0539P)^2 + 1.1322P$, where $P = (F_o^2 + 2F_c^2)/3$).

5. Supplementary material available

Additional crystallographic data for compounds **1**, **2**, **4** and **5** are available on request from Fachinformationszentrum Karlsruhe, D-76344 Eggenstein-Leopoldshafen 2, upon quotation of the depository numbers 405689, 405695, 405957 and 405688, the names of the authors and the journal reference for this article.

Acknowledgements

Financial support of this work by funds of the University of Konstanz is gratefully acknowledged. We thank Dr. A. Geyer and M. Cavegen for the 2D-ROESY measurements.

References

[1] M. Hüttenhofer, M.-H. Prosenc, U. Rief, F. Schaper and H.H. Brintzinger, *Organometallics, 15* (1996) 4816.

[2] D. Steinborn and R. Taube, *J. Organomet. Chem., 284* (1985) 395; R. Taube and L. Krukowa, *J. Organomet. Chem., 347* (1988) C9; D. Steinborn, I. Wagner and R. Taube, *Synthesis, 4* (1989) 304; D. Steinborn, B. Thies, I. Wagner and R. Taube, *Z. Chem., 29* (1989) 333; R. Taube and K. Seyferth, *Z. Chem., 14* (1974) 410; *J. Organomet. Chem., 111* (1976) 215; K. Seyferth and R. Taube, *J. Organomet. Chem., 268* (1984) 155.

[3] K.L.T. Wong and H.H. Brintzinger, *J. Am. Chem. Soc., 97* (1975) 5143.

[4] M.L.H. Green and C. Giannotti, *J. Chem. Soc., Chem. Commun.*, (1972) 1114; J. Okuda and G.E. Herberich, *Organometallics, 6* (1987) 2331; G.E. Herberich, W. Barlage and K. Linn, *J. Organomet. Chem., 414* (1991) 193.

[5] E.O. Fischer and H.P. Kögler, *Angew. Chem., 68* (1956) 462; E.O. Fischer, K. Ulm and H.P. Fritz, *Chem. Ber., 93* (1960) 2167; E.O. Fischer and K. Ulm, *Chem. Ber., 95* (1962) 692.

[6] J.L. Robbins, N. Edelstein, B. Spencer and J.C. Smart, *J. Am. Chem. Soc., 104* (1982) 1882; J.L. Robbins, *Dissertation*, University of California, Berkeley, 1981.

[7] J. Darkwa, J.F. Richardson and T.S. Soerensen, *Acta Crystallogr., C46* (1990) 745.

[8] F.W.S. Benfield and M.L.H. Green, *J. Chem. Soc., Dalton Trans.*, (1974) 1324; R.L. Cooper and M.L.H. Green, *J. Chem. Soc. (A)*, (1967) 1155 and references cited therein.

[9] M. Moràn and V. Fernàndez, *J. Organomet. Chem., 165* (1979) 215; M. Moràn, *Trans. Met. Chem., 6* (1981) 173; M. Moràn and M. Gayoso, *Z. Naturforsch., 38b* (1983) 177; *J. Organomet. Chem., 243* (1983) 423.

[10] H. Schwemlein, L. Zsolnai, G. Huttner and H.H. Brintzinger, *J. Organomet. Chem., 256* (1983) 285.

[11] G. Huttner, H.H. Brintzinger, L.G. Bell, P. Friedrich and D. Neugebauer, *J. Organomet. Chem., 145* (1978) 329.

[12] K.M. Simpson, M.F. Rettig and R.M. Wing, *Organometallics, 11* (1992) 4363.

[13] E.U. van Raaij and H.H. Brintzinger, *J. Organomet. Chem., 356* (1988) 315.

[14] E.U. van Raaij, H.H. Brintzinger, L. Zsolnai and G. Huttner, *Z. Anorg. Allg. Chem., 577* (1989) 217.

[15] P. Jutzi and R. Dickbreder, *Chem. Ber., 119* (1986) 1750; P. Jutzi, D. Kanne, M. Hursthouse and A.J. Howes, *Chem. Ber., 121* (1988) 1299.

[16] C.M. Fendrick, E.A. Mintz, L.D. Schertz, T.J. Marks and V.W. Day, *Organometallics, 3* (1984) 819; C.M. Fendrick, L.D. Schertz, V.W. Day and T.J. Marks, *Organometallics, 7* (1988) 1828.

[17] F. Wochner, L. Zsolnai, G. Huttner and H.H. Brintzinger, *J. Organomet. Chem., 288* (1985) 69.

[18] D.M.J. Foo and P. Shapiro, *Organometallics, 14* (1995) 4957.

[19] E.O. Fischer and K. Ulm, *Z. Naturforsch., 15b* (1960) 59; *Chem. Ber., 94* (1961) 2413.

[20] H. Köpf and J. Pickardt, *Z. Naturforsch., 36b* (1981) 1208; K.P. Reddy and J.L. Petersen, *Organometallics, 8* (1989) 2107.

[21] M. Bochmann, S.J. Lancaster, M.B. Hursthouse and M. Mazid, *Organometallics, 12* (1993) 4718; G.M. Diamond, M.L.H. Green, P. Mountford, N.A. Popham and A.N. Chernega, *J. Chem. Soc., Chem. Commun.*, (1994) 103.

[22] O. Koch, F. Edelmann, B. Lubke and U. Behrens, *Chem. Ber., 115* (1982) 3049.

[23] F.G.N. Cloke, J.P. Day, J.C. Green, C.P. Morley and A.C. Swain, *J. Chem. Soc., Dalton Trans.*, (1991) 789; F.G.N. Cloke, J.C. Green, M.L.H. Green and C.P. Morley, *J. Chem. Soc., Chem. Commun.*, (1985) 945; J.E. Bercaw, *J. Am. Chem. Soc., 96* (1974) 5087; J.E. Bercaw, R.H. Marvich, L.G. Bell and H.H. Brintzinger, *J. Am. Chem. Soc., 94* (1972) 1219; H. Brunner, G. Gehart, W. Meier, J. Wachter and T. Burgemeister, *J. Organomet. Chem., 493* (1995) 163.

[24] G. Michael, J. Kaub and C.G. Kreiter, *Angew. Chem., 97* (1985) 503.

[25] P. Selg, *Dissertation*, Universität Konstanz, 1996.

[26] L.R. Field, E. Wilhelm and R. Battino, *J. Chem. Thermodynam., 6* (1974) 237; E.U. van Raaij, C.D. Schmulbach and H.H. Brintzinger, *J. Organomet. Chem., 328* (1987) 275.

[27] H.G. Schuster-Woldan and F. Basolo, *J. Am. Chem. Soc., 88* (1966) 1657; M.E. Rerek and F. Basolo, *Organometallics, 2* (1983) 372; *J. Am. Chem. Soc., 106* (1984) 5908.

[28] F.H. Köhler and W. Prössdorf, *Z. Naturforsch., 32b* (1977) 1026.

[29] K. Handlíř, J. Holeček and J. Klikorka, *Z. Chem., 19* (1979) 266.

[30] F.X. Kohl and P. Jutzi, *J. Organomet. Chem., 243* (1983) 119 and references cited therein.

[31] G. Schmitt and S. Özmann, *Chem. Zeit., 100* (3) (1976) 143.

[32] G.M. Sheldrick, SHELXTL-PLUS, University of Göttingen, 1986; SHELXL-93, University of Göttingen, 1993.